The Role Played by Mass, Friction, and Inertia on the Driving Torques of Lower-Limb Gait Training Exoskeletons

Rafhael M. Andrade, *Member, IEEE*, and Paolo Bonato, *Senior Member, IEEE*

***Abstract*—Lower-limb gait training exoskeletons are extraordinary tools used to reduce the burden of locomotor impairments in patients with neurological diseases. However, the transparent operation and backdrivability of such systems still needs to be improved. Moreover, it is not completely understood how the mechanical design of the robot can interfere with the user's gait pattern. Aiming to address these shortcomings, we investigate the required driving torques and mechanical power to move the legs under a wide range of actuator's mass, inertia and friction and thigh/shank lengths. We used the ExoRoboWalker, a six-degree-of-freedom lower-limb exoskeleton, to build a framework model based on the double-pendulum approach integrated with the actuators' mechanical impedance. Decoupled joint apparent inertia and the Rayleigh's dissipation function were introduced to the robot's Lagrangian to consider the effects of gearhead ratio and joint friction in the model. Firstly, it is presented the isolated effect of such variables on the required driving torques of the system. The oscillation frequency for the minimum joint torque was severely affected by variations of inertia, friction, and links length. Secondly, the combined effect of the actuator's mass, inertia and friction reveled that a heavier exoskeleton with low-ratio transmission required less torque and mechanical power than a lighter one with greater reduction ratio depending on the oscillation frequency, which is remarkable. These findings have important implications for new designs of lower-limb gait training systems.**

***Index Terms*—Lower-limb exoskeleton, mechanical impedance, gait rehabilitation, joint torque, mechanical power.**

I. Introduction

THE NUMBER of lower-limb exoskeleton designs for rehabilitation has grown over the past two decades [1]. Gait training exoskeletons can be divided in two main groups: treadmill-based systems and overground gait training devices [2]. Treadmill-based exoskeletons, like Lokomat (Hocoma AG, Switzerland), are lower-limb wearable robots with a fixed structure mounted over a treadmill used to assist the user to find a physiological gait pattern [3]. Overground gait training exoskeletons, on the other hand, such as Indego (Parker Hannifin Corp., USA) [4], HAL (Cyberdyne Inc., Japan) [5], Ekso (Ekso Bionics, USA) [6], Atalante (Wandercraft, France) and others [7], can assist the user to walk while challenging their balance control system [8]. In this case, the weight of the system is carried by the user.

To improve the outcomes of the lower-limb gait training robots and following the assistance as needed concept [9], the system should be "transparent" to the user and just introduce perturbations to correct the gait when voluntarily generated motor outputs deviate significantly from the physiological gait [10]. However, the development of a transparent operation mode is still an open problem with several implementation challenges [11], [12]. Overground gait trainers should be as light as possible to reduce the burden of bearing the system. On the other hand, lightweight actuators require high-ratio transmission to improve the torque density of the system, resulting in joints with high friction and apparent inertia, i.e., high impedance actuators with reduced backdrivability [13], [14]. This requirement for highly transparent exoskeletons has been addressed in different ways among research groups. The effect of adding masses on the user's legs [15], [16] or exoskeleton [17] on the gait kinematics has been investigated as the most important criterion to design transparent lower-limb exoskeletons [15], [18]. Then, some designs of exoskeleton actuators prioritize low mass and high torque density [19]–[21]. At the same time, to improve the system's compliance and volitional motion of the user, some research groups prioritize actuators with low impedance and high backdrivability [22]–[25].

Indeed, an external structure with significant mass and inertia attached to the legs can unwantedly modify the gait kinematics and dynamics, spaciotemporal parameters, and metabolic cost of walking [26] and negatively interfere with the rehabilitation process. During the gait, conservative potential and kinetic energy of the limbs' mass and inertia and elastic energy stored in muscles and tendons are interchanged in a complex way to minimize the energy cost of walking [27]. To investigate how extra weight attached to the legs interferes with gait kinematics, Holt *et al.* [28] used the simple-pendulum

Manuscript received August 26, 2020; revised October 25, 2020 and December 11, 2020; accepted January 2, 2021. Date of publication January 18, 2021; date of current version February 22, 2021. This article was recommended for publication by Associate Editor A. Forner-Cordero and Editor P. Dario upon evaluation of the reviewers' comments. This work was supported in part by the Fundação de Amparo à Pesquisa e Inovação do Espírito Santo (FAPES, TO 207/2018) under Project 83276262, and in part by the Peabody Foundation. *(Corresponding author: Rafhael M. Andrade.)*

Rafhael M. Andrade is with the Department of Mechanical Engineering, Universidade Federal do Espirito Santo, Vitória 29075-910, Brazil, and also with the Department of Physical Medicine and Rehabilitation, Harvard Medical School, Spaulding Rehabilitation Hospital, Charlestown, MA 02129 USA (e-mail: rafhael.andrade@ufes.br).

Paolo Bonato is with the Department of Physical Medicine and Rehabilitation, Harvard Medical School, Spaulding Rehabilitation Hospital, Charlestown, MA 02129 USA (e-mail: pbonato@mgh.harvard.edu).

Digital Object Identifier 10.1109/TMRB.2021.3052014

model with the same mass of the leg and equivalent length of the leg's center of mass (CoM) to predict the self-selected stride frequency. The authors observed that the participant naturally adjusts their stride frequency to the resonant frequency of the equivalent pendulum to minimize the hip mechanical power and the energetic cost of walking. Browning *et al.* [16] and Jin *et al.* [17] investigated the effect of adding mass to the subject's legs [16] or to the exoskeleton's structure [17] and found an increasing trend in stride time, but no significant changes in joint angles of the user. On the other hand, Rossi *et al.* [15] did not find significant differences in the gait parameters of children when adding up to 2.5 kg of extra weight to their legs. Even not completely understood, the position of the added mass plays an important role on the resultant gait kinematics [26]. Moreover, the effect of joint friction on the gait can be somehow equivalent to the drag forces produced by walking in water. Barela *et al.* [32] investigate the implication of walking in water on the gait kinematics. The authors noted that to minimize the gait cost in this condition, the subjects reduce their walking speed by dropping the stride frequency but preserving the step length and joint angles when compared with walking on land.

Since mass, friction and inertia play a role on the self-selected stride frequency, employing a transparent operation strategy that just minimizes the interaction force with the user [12], [33], [34] is not enough to avoid interfering with the user's kinematics. Moreover, despite research in the area, it is not clear how the actuator's impedance, i.e., its mass, friction and apparent inertia created by the gearhead ratio, affects the driving torques, natural step frequency, and mechanical power of lower-limb exoskeletons and how it can interfere with the user's gait. Bartenbach *et al.* [35] built a lower-limb exoskeleton platform to investigate the effect of the robot's mechanical design on the user's gait kinematics, but no result was reported regarding the effect of mass, inertia, friction and stride frequency. We suppose that for a long-term gait rehabilitation, the system should help the user find a physiological gait pattern with lower metabolic cost than their pathological condition [36]. For that reason, the system's design should take into account the stride frequency of the minimal required mechanical power of the joints. To address these assumptions, in this article we investigate the joint driving torques and mechanical power of lower-limb gait training exoskeletons under a wide range of actuator's mass, apparent inertia and transmission ratio variation based on a model of the ExoRoboWalker [13], a six degree-of-freedom lower-limb exoskeleton for overground gait training. As it would not be feasible to perform these experiments on the physical prototype, we modelled the exoskeleton as a double-pendulum and integrated the actuator's impedance, which consists of joint apparent inertia and friction, by introducing the Rayleigh's dissipation function into the robot's Lagrangian. The complete approach is presented in the Section II. In the Section III, our data is displayed in terms of driving torques and mechanical power against the leg oscillation frequency (ω) ranging from 0.1 to 10 rad/s. In the Section IV, we argue how these variables can interfere with the user's gait.

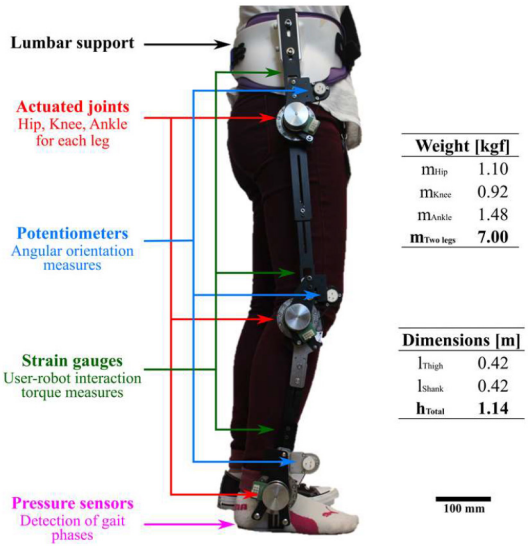

Fig. 1. The ExoRoboWalker mechanics is composed by six small actuators mounted on the hip, knee and ankle joints joined by lateral bars, lumbar support, and insoles.

II. Methodology

A. The ExoRoboWalker

The ExoRoboWalker, shown in Fig. 1, is an overground gait rehabilitation trainer designed to assist movements of the hip, knee, and ankle joints on the sagittal plane. The exoskeleton configuration consists of six small lightweight harmonic-drive based actuators mounted on the hip, knee and ankle, which are joined by lateral bars to the thigh, leg, and foot (support and insole). Each actuator is composed by an EC 45 flat, (70 watts, brushless, Maxon Motors, Switzerland) and a CSD-20-160-2a harmonic-drive (HD) (reduction ratio of 160, Harmonic Drive LLC, Massachusetts, USA), whose mass is displayed in the figure. The standard lengths of the thigh and shank links used in this study are 0.42 m, but it can be adjusted to fit a wide range of leg lengths.

B. ExoRoboWalker Model

To investigate the effects of varying the actuator's mass, inertia, and friction on the driving torques and mechanical power using the physical prototype of the ExoRoboWalker becomes unfeasible, in view of the wide range of actuator sizes, motorization and transmission ratio to be tested. To make such an analysis possible, we built a complete dynamic model in MATLAB environment (MathWorks Inc, Massachusetts, EUA) using the real properties of the ExoRoboWalker and the data from its parts catalog.

To build a complete dynamic model of the ExoRoboWalker, we considered the robot's leg behaves like a double-pendulum integrated to the actuator's impedance. The double-pendulum is a simple physic system that can display a complex dynamic. It is the most used approach to model lower-limb exoskeleton dynamics [37], [38]. However, the double-pendulum modeling does not consider the joint friction and apparent inertia created by the gearhead ratio, but just the joint mass. To take in to account the actuator's properties in the model, firstly, we

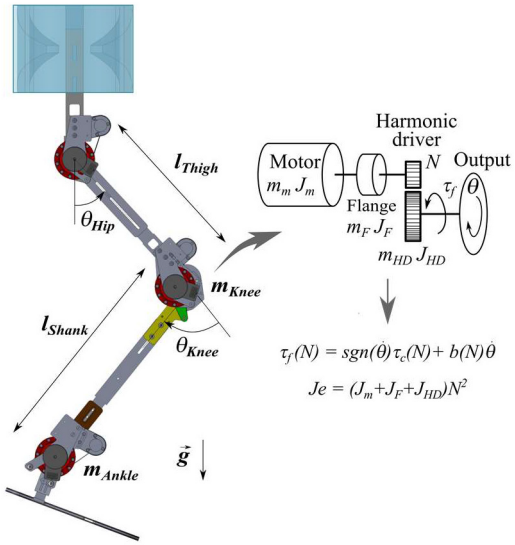

Fig. 2. ExoRoboWalker approached to the double-pendulum model integrated with the actuator's impedance. $l_{Thigh} = l_1, l_{Shank} = l_2, \theta_{Hip} = \theta_1, \theta_{Knee} = \theta_2, m_{Knee} = m_1$ and $m_{Ankle} = m_2$. The actuator consists of an EC motor (inertia $= J_m$), flange (inertia $= J_F$), and an harmonic-drive (HD) (inertia $= J_{HD}$). The actuator friction is approached to the coulomb (τ_c) plus viscous friction model ($b\dot{\theta}$) as a function of the HD reduction ratio (N).

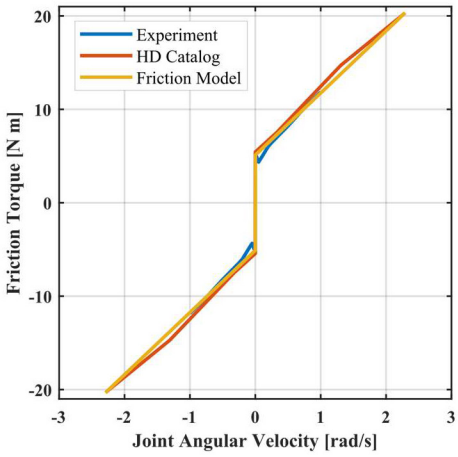

Fig. 3. Comparison of the frictional torque on the exoskeleton joint (blue line), friction from the harmonic-drive catalog (red line), and the proposed friction model (yellow line) for transmission ratio 160.

modelled the actuator's dynamics as a function of the transmission ratio (N), considering the apparent inertia and friction, as shown in Fig. 2. Then, we introduced the actuator's apparent inertia to the robot's kinetic energy and the joint friction to the ideal double-pendulum Lagrangian using the Rayleigh's dissipation function [41].

The apparent inertia of the actuator ($Je = 0.745$ kg.m^2) can be calculated by (1), where $J_m = 1.81\text{E}-05$ kg.m^2 and $J_{HD} = 9.00\text{E}-06$ kg.m^2 are the motor and HD inertia taken from the suppliers catalog, respectively. $J_F = 2.0\text{E}-06$ kg.m^2 is the gearbox adapter inertia and $N = 160$ is the HD transmission ratio.

$$Je = (J_m + J_{HD} + J_F)N^2 \tag{1}$$

As the HD is the main responsible for the friction effect on the exoskeleton [13], we employed data from the CSD-20-2a harmonic-drive series Catalog (Harmonic Drive LLC, Massachusetts, USA) to model the actuator's friction. We expanded the widely used Coulomb plus viscous friction model [11], [12], [39] as a function of the gearhead ratio according (2). Fig. 3 presents the comparison of the proposed model (yellow line), with the frictional torque according to the supplier catalog (red line), and the measured torque friction of the joints for reduction ratio $N = 160$ (blue line). The joint friction was gathered by measuring the required torque to turn the isolated joint without the links for different controlled angular velocities.

$$\begin{cases} \tau_f(N) = \tau_C(N)sgn(\dot{\theta}) + b(N)\dot{\theta} \\ \tau_C(N) = 2.67 + 0.0167N \\ b(N) = 0.0003N^2 - 0.0064N - 0.0079 \end{cases} \tag{2}$$

where τ_f is the frictional torque of the joint as a function of the reduction ratio N, τ_C is the Coulomb friction, and b is the viscous friction coefficient.

As the actuators mass of the ExoRoboWalker are centered at the joints and the links l_{Thigh} and l_{Shank} are lightweight, we assume that the double-pendulum model has masses m_1 and m_2 concentrated at the end of the links l_1 and l_2, respectively. The robot's equation of motion can be expressed as:

$$\tau = M(\theta)\ddot{\theta} + C(\theta, \dot{\theta})\dot{\theta} + G(\theta) + F(N, \dot{\theta}) \tag{3}$$

where τ is the required torque to move the joints, θ is the relative angle of the links l_1 and l_2, M is the mass matrix, C is the Coriolis and centrifugal matrix, G is the gravitational matrix, and $F(N)$ is the frictional torques matrix of the exoskeleton as a function of N. Equation (3) can be derived through the Lagrange's equations [40] incorporated with the dissipative forces [41] as:

$$\tau_i = \frac{d}{dt}\left(\frac{\partial L}{\partial \dot{\theta}_i}\right) - \frac{\partial L}{\partial \theta_i} + \frac{\partial R(N)}{\partial \dot{\theta}_i} - \xi_i^{(nc)}(N) \tag{4}$$

where L is the exoskeleton's Lagrangian function (5), which can be derived from the total kinetic energy of the system, T (6), and the total potential energy, V (7).

Since the transmission ratio (N) can vary independently of the gearhead mass and inertia, we can have different joint apparent inertia (Je), given by (1), for the same actuator's mass. To investigate the independent effect of inertia on the exoskeleton's dynamics, the actuator's apparent inertia is considered decoupled from the actuator's mass. It is done by introducing the kinetic energy of the joint apparent inertia, $\frac{1}{2}\text{Je}\dot{\theta}^2$, on T (6). R (8) is the Rayleigh's dissipation function, which takes into account just the viscous friction term of τ_f. $\xi_i^{(nc)}(N)$ (9) includes all generalized non-conservative forces not considered by the Rayleigh's term, i.e., the Coulomb friction term.

$$L = T - V \tag{5}$$

$$\begin{aligned} T = {} & \frac{1}{2}\left(m_1 l_1^2 + Je_1\right)\dot{\theta}_1^2 + \frac{1}{2}\left(m_2 l_2^2 + Je_2\right)\dot{\theta}_2^2 \\ & + \frac{1}{2}m_2\Big[\left(l_1^2 + 2l_1 l_2 cos\theta_2 + l_2^2\right)\dot{\theta}_1^2 \\ & - 2\left(l_1 l_2 cos\theta_2 + l_2^2\right)\dot{\theta}_1\dot{\theta}_2\Big] \end{aligned} \tag{6}$$

$$V = -(m_1 + m_2)gl_1 cos\theta_1 \; - m_2 g l_2 cos(\theta_1 - \theta_2) \tag{7}$$

$$R(N) = \frac{1}{2}\sum_i b(N)_i \dot{\theta}_i^2 \tag{8}$$

$$\xi_i^{(nc)}(N) = -\; \tau_{Ci}(N) sgn\big(\dot{\theta}_i\big) \tag{9}$$

where $m_1 = m_{Knee}, m_2 = m_{Ankle}, l_1 = l_{Thigh}, l_2 = l_{Shank}, \theta_1 = \theta_{Hip}$, and $\theta_2 = \theta_{Knee}$.

Then, considering the complete model of the ExoRoboWalker, the terms M, C, G, and F of (4) can be calculated as follows:

$$M = \begin{bmatrix} (m_1 + m_2)l_1^2 + Je_1 + \ldots & -m_2\big(l_1 l_2 cos\theta_2 + l_2^2\big) \\ +m_2\big(2l_1 l_2 cos\theta_2 + l_2^2\big) & \\ -m_2\big(l_1 l_2 cos\theta_2 + l_2^2\big) & m_2 l_2^2 + Je_2 \end{bmatrix} \tag{10}$$

$$C = \begin{bmatrix} -2m_2 l_1 l_2 sin\theta_2 \dot{\theta}_2 & m_2 l_1 l_2 sin\theta_2 \dot{\theta}_2 \\ m_2 l_1 l_2 sin\theta_2 \dot{\theta}_1 & 0 \end{bmatrix} \tag{11}$$

$$G = \begin{bmatrix} (m_1 + m_2)l_1 g sin\theta_1 + m_2 l_2 g sin(\theta_1 - \theta_2) \\ -m_2 l_2 g sin(\theta_1 - \theta_2) \end{bmatrix} \tag{12}$$

$$F = \begin{bmatrix} \tau_{C1}(N) sgn\big(\dot{\theta}_1\big) \; + \; b_1(N)\dot{\theta}_1 \\ \tau_{C2}(N) sgn\big(\dot{\theta}_2\big) \; + \; b_2(N)\dot{\theta}_2 \end{bmatrix} \tag{13}$$

To generalize the analysis, our main data is displayed in terms of magnitude joint torque using as reference the joint torques of the ideal double-pendulum model. Let $\hat{\tau}$ be the dynamic torques generated by the inertial, Coriolis, and gravitational forces of the ideal double-pendulum as follows:

$$\widehat{\tau} = \widehat{M}(\theta)\ddot{\theta} + C\big(\theta, \dot{\theta}\big)\dot{\theta} + G(\theta) \tag{14}$$

where $\widehat{M}$ is the mass matrix of the idealized exoskeleton. As joint inertia and friction do not change the Coriolis/centrifugal and gravitational matrixes, C and G are given by (11) and (12), respectively. Equation (14) can be derived through Lagrange's equation as follows:

$$\widehat{\tau}_i = \frac{d}{dt}\left(\frac{\partial \hat{L}}{\partial \dot{\theta}_i}\right) - \frac{\partial \hat{L}}{\partial \theta_i} \tag{15}$$

where $\widehat{L}$ is the ideal double-pendulum Lagrangian function and can be calculated by $\hat{L} = \widehat{T} \; - \hat{V}$. In this case, the total kinetic energy of the system, $\widehat{\mathrm{T}}$, is given by (16) and the total potential energy, $\widehat{V}$, is the same of V (7), which results in $\widehat{M}$ as follows:

$$\hat{T} = \frac{1}{2}m_1 l_1^2 \dot{\theta}_1^2 + \frac{1}{2}m_2\Big[\Big(l_1^2 + 2l_1 l_2 cos\theta_2 \; + l_2^2\Big)\dot{\theta}_1^2 - 2\Big(l_1 l_2 cos\theta_2 \; + l_2^2\Big)\dot{\theta}_1\dot{\theta}_2 + l_2^2\dot{\theta}_2^2\Big] \tag{16}$$

$$\widehat{M} = \begin{bmatrix} (m_1 + m_2)l_1^2 + \ldots & -m_2\big(l_1 l_2 cos\theta_2 + l_2^2\big) \\ +m_2\big(2l_1 l_2 cos\theta_2 + l_2^2\big) & \\ -m_2\big(l_1 l_2 cos\theta_2 + l_2^2\big) & m_2 l_2^2 \end{bmatrix} \tag{17}$$

The magnitude joint torque of the proposed model, which considers the joint torques of the ideal double-pendulum as reference, is given by (18).

$$\tau_{dB} = 20log_{10}\frac{max(\tau_i) - min(\tau_i)}{max(\widehat{\tau}_i) - min(\widehat{\tau}_i)} \tag{18}$$

As the amount of swing leg work is quite significant for the metabolic cost of walking [29], [42], we used in our analysis a sinusoidal input θ_1 angle ranging from $-20°$ to $20°$ degrees with phase $\varphi = 180°$ and θ_2 angle ranging from 0 to 65° to simulate the leg movement during swing-phase. Angular velocity ($\dot{\theta}_i$) and acceleration ($\ddot{\theta}_i$) were calculated using discrete time (t_n) derivative function as follows:

$$\dot{\theta}_i = \frac{d\theta_i}{dt} = \frac{\theta_i^{t_n} - \theta_i^{t_{n-1}}}{t_n - t_{n-1}} \tag{19}$$

$$\ddot{\theta}_i = \frac{d\dot{\theta}_i}{dt} = \frac{\dot{\theta}_i^{t_n} - \dot{\theta}_i^{t_{n-1}}}{t_n - t_{n-1}}. \tag{20}$$

III. Results

Mass, inertia, friction, and dimensions play an important role on the driving torques and mechanical power of lower-limb exoskeletons as well as on the user's kinematics. The effect of such variables can sorely vary depending on the oscillation frequency of the robot's legs and, consequently, on the gait training selected speed. To address such an outcome, here we present the results in two main categories. Firstly, the isolated effects of a single of those variables are investigated. Secondly, the combined effects of actuator's mass, friction, and inertia variation are considered.

To improve the generalization, our main data is displayed in terms of magnitude joint torque [dB], according to (18), joint torque [N m] or mechanical power [W] against the leg oscillation frequency (ω) ranging from 0.1 to 10 rad/s.

A. Isolated Effects

To investigate the isolated effect of friction, we display in Fig. 4 the magnitude torque [dB] as a function of ω for motor-reducer transmission ratio ranging from N=30 to N=160, and considering $Je_1 = Je_2 = 0, m_1 = m_{K_{nee}}$ and $m_2 = m_{Ankle}, l_1 = l_{Thigh}$ and $l_2 = l_{Shank}$. $\hat{\omega}_{1\mathrm{n}}$ and $\hat{\omega}_{2\mathrm{n}}$ represent the resonant frequency of the ideal double-pendulum. The magnitude torque is greater as N increases and rises fast when ω approaches to the $\hat{\omega}_{\mathrm{n}}$. Due to the greater conservative forces acting on the hip joint, it is less sensitive to friction, so that the magnitude torques of the knee joint are greater than the hip ones. Regarding the isolated effect of changing the actuator's mass, as expected, a proportionally greater torque is required to move the joints for increased actuator's mass and no variation on the natural oscillation frequency is observed, so the results are not shown here.

Fig. 5 shows the isolated effect of the actuator's apparent inertia variation on the magnitude joint torques, considering $\tau_f = 0, l_1 = l_{Thigh}$, and $l_2 = l_{Shank}$, $m_1 = m_{K_{nee}}$, and $m_2 = m_{Ankle}$. Red line is the magnitude torque for $Je_1 = Je_{Hip}, Je_2 = Je_{Knee}$, blue line for half the apparent joint inertia and yellow line for double inertia. No significant variation in the magnitude torques is observed when the oscillation frequency is below 0.6 rad/s. However, the magnitude torque falls when ω is close to the corresponding resonant frequency of the exoskeleton's model and rises for $\omega \sim \hat{\omega}_{\mathrm{n}}$, i.e., the natural oscillation frequency of the system decreases as the joint apparent inertia increases. Moreover, the magnitude torque is greater than zero for $\omega > \hat{\omega}_{\mathrm{n}}$, mainly for the

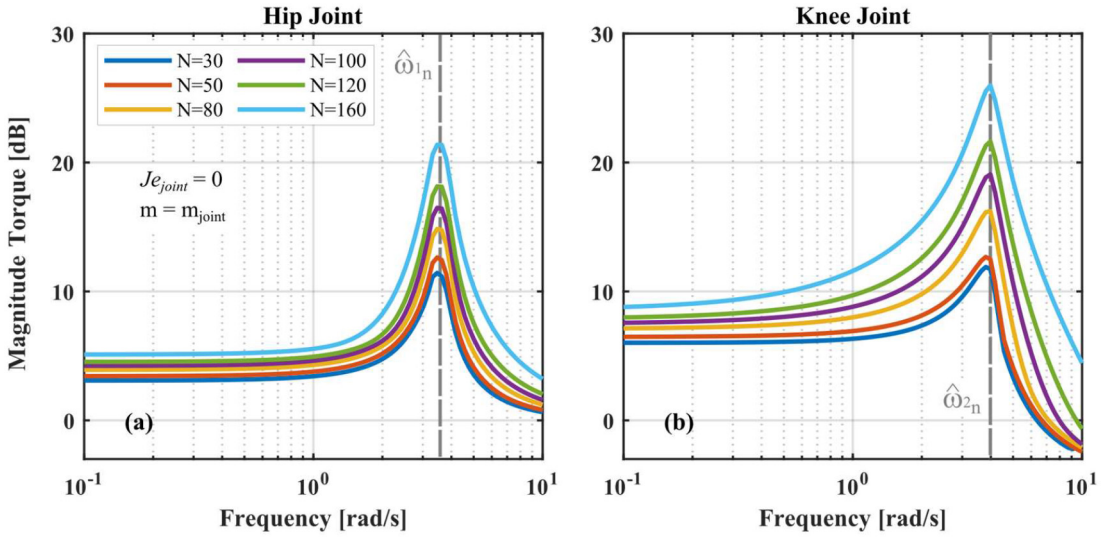

Fig. 4. Isolated effect of the actuator friction as a function of the motor-reducer transmission ratio on the magnitude torque (dB). $\hat{\omega}_{1n}$ represents the resonant frequency of the ideal double-pendulum on the hip joint (a) and $\hat{\omega}_{2n}$ for the knee joint (b).

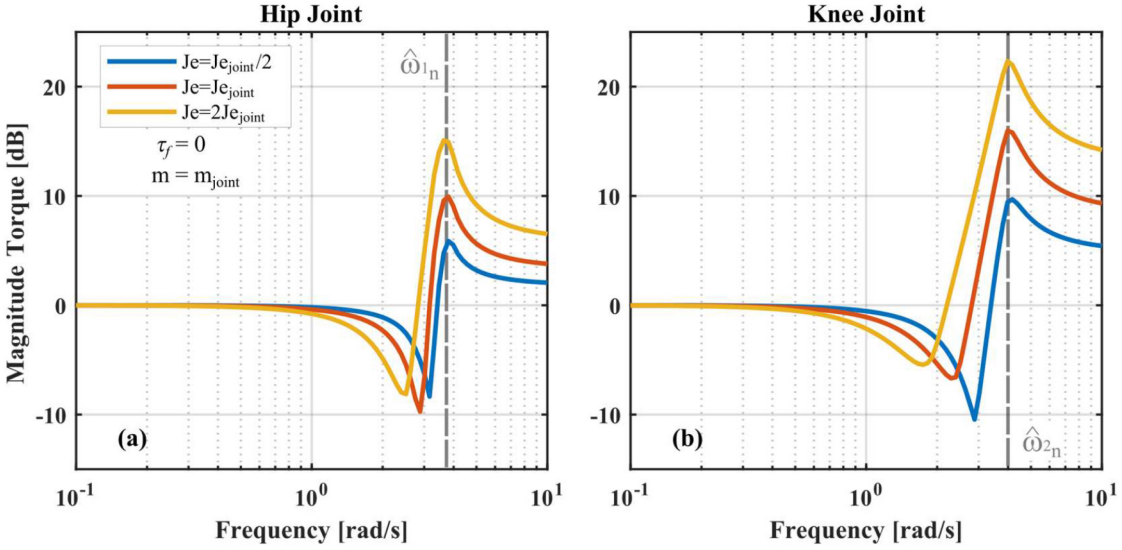

Fig. 5. Isolated effect of the joint apparent inertia (Je) on the magnitude torque (dB). $\hat{\omega}_{1n}$ represents the hip joint (a) resonant frequency of the double-pendulum model disregarding joint impedance and $\hat{\omega}_{2n}$ for the knee joint (b).

knee joint, in which the effect of the system's mass is less important.

Finally, Fig. 6 shows the magnitude torque of the hip and knee joint against ω for a range of links length, considering $\tau_f = 0, Je_1 = Je_2 = 0, m_1 = m_{K_{nee}}$, and $m_2 = m_{Ankle}$. We performed three sets of simulations: varying l_1 ($l_1 = l_{Thigh}/2$ and $2l_{Thigh}$) whereas $l_2 = l_{Shank}$, represented by blue and red lines; varying $l_2 (l_2 = l_{Shank}/2$ and $2l_{Shank})$ whereas $l_1 = l_{Thigh}$, yellow and purple lines; and finally, for $l_1 = l_{Thigh}/2$ and $l_2 = l_{Shank}/2$, and $l_1 = 2l_{Thigh}$ and $l_2 = 2l_{Shank}$, green and light blue lines, respectively. As expected, increased links length requires greater torque on the joints. Moreover, the links length variation induces different resonant frequencies in the system. Furthermore, changing the length of the shank plays a more important role on the hip and knee torques than varying the thigh length. Combined effects of change the thigh and shank links length play a more important role on the joint torques than the variation of a link individually.

To compare the isolated effects of friction, inertia, and links length variation, Fig. 7 presents the frequency of minimum magnitude torque as a function of the gearhead ratio (R) of each variable. The friction effect (shown as $N = 100R$) produces a minimum magnitude torque just on the knee joint, that's why it is not shown on the hip joint graph. Introducing joint inertia or increasing the links length reduces the system's resonant frequency, thereby determining a minimum magnitude torque in a frequency below $\hat{\omega}_n$. However, although the increased friction on the joints (denoted by increased N) requires high torque from the hip and knee actuators, for high frequencies ($\omega > 6$ rad/s), the increased joint friction helps to brake the inertial and Coriolis forces driven by the thigh movement on the shank [23]. In other words, in

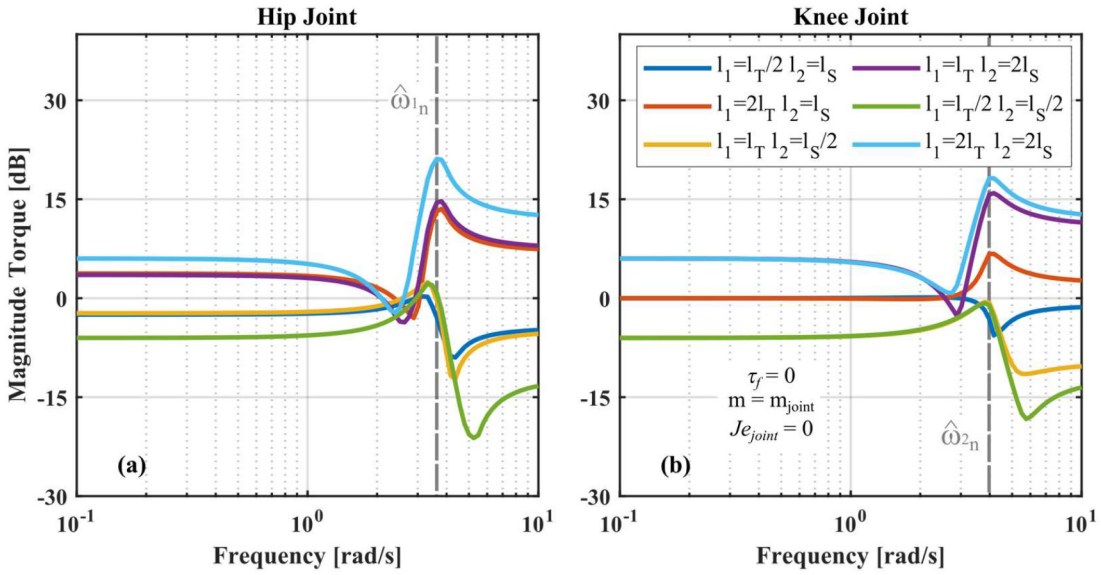

Fig. 6. Isolated effect of the exoskeleton's link length on the magnitude torque (dB). $l_T = l_{Thigh}$ and $l_S = l_{Shank}$ for short. $\hat{\omega}_{1n}$ represents the resonant frequency of the ideal double-pendulum model on the hip joint (a) and $\hat{\omega}_{2n}$ for the knee joint (b).

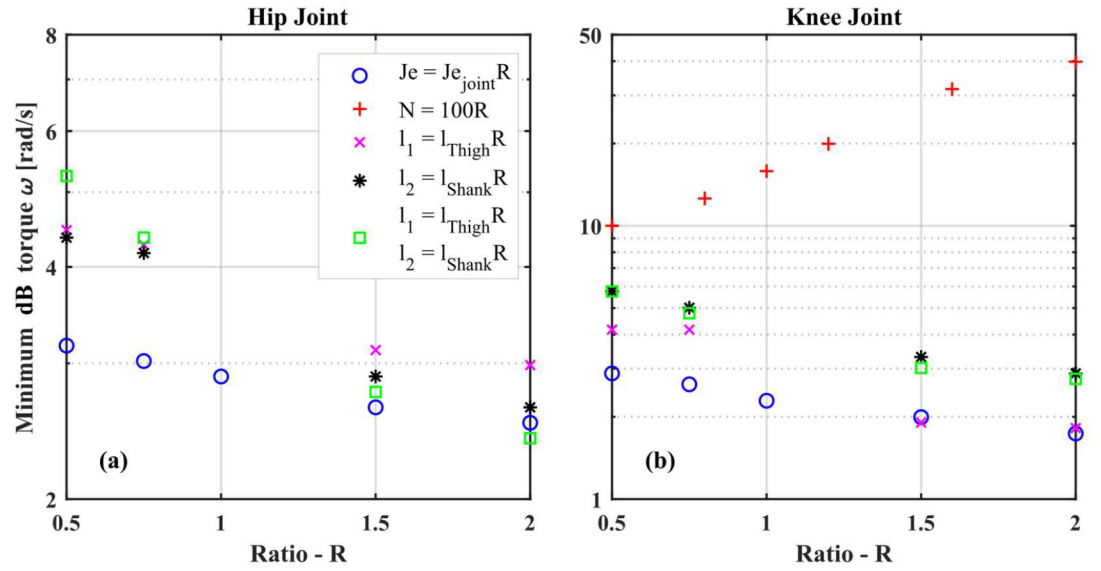

Fig. 7. Variation in oscillation frequency (ω) for the minimum value of joint torque as a function of the isolated effects of apparent inertia (Je), friction due to gearhead ratio (N), and exoskeleton's links length (l_1 and l_2). (a) hip joint and (b) knee joint.

high frequencies, friction minimizes the out-of-phase effects of inertia and Coriolis forces from the hip movement on the knee joint.

B. Combined Effects

Here we present the combined effects of friction, inertia, and mass on the driving torques and mechanical power of lower-limb exoskeletons. The effect of the actuator's mass variation is shown in Fig. 8. The results are gathered considering the standard reduction ratio ($N = 160$) and link length ($l_1 = l_{Thigh}$ and $l_2 = l_{Shank}$) of the ExoRoboWalker, and just varying the actuator's mass as: $m_1 = m_{K_{nee}}$ and $m_2 = m_{Ankle}$, red line (standard), $m_1 = 2m_{K_{nee}}$ and $m_2 = 2m_{Ankle}$, yellow line and $m_1 = m_{K_{nee}}/2$ and $m_2 = m_{Ankle}/2$, blue line. Fig. 8(a) and (b) are the magnitude torque in dB of the hip and knee joints, respectively. The magnitude torque is greater than zero for all frequency ranges tested. No minimum magnitude torque is observed due to the high friction of the actuator. Fig. 8 (c) and (d) are the required torque to move the joints; and lastly, Fig. 8 (e) and (f) are the resulting mechanical power of the joints. Increased actuator's mass results in greater magnitude torque, as expected. However, no significant difference is observed for the magnitude torque for $\omega \sim \hat{\omega}_n$, because friction and inertia do not change, but just the actuator's mass. Regarding the joint torque, the actuator's friction becomes less important as the actuator's mass increases and, curiously, for $\omega = 4$ to 8 rad/s on the knee joint, a greater actuator's mass required less torque than the lighter one. The greater inertia of the link, resulted from the increased mass, overcomes the

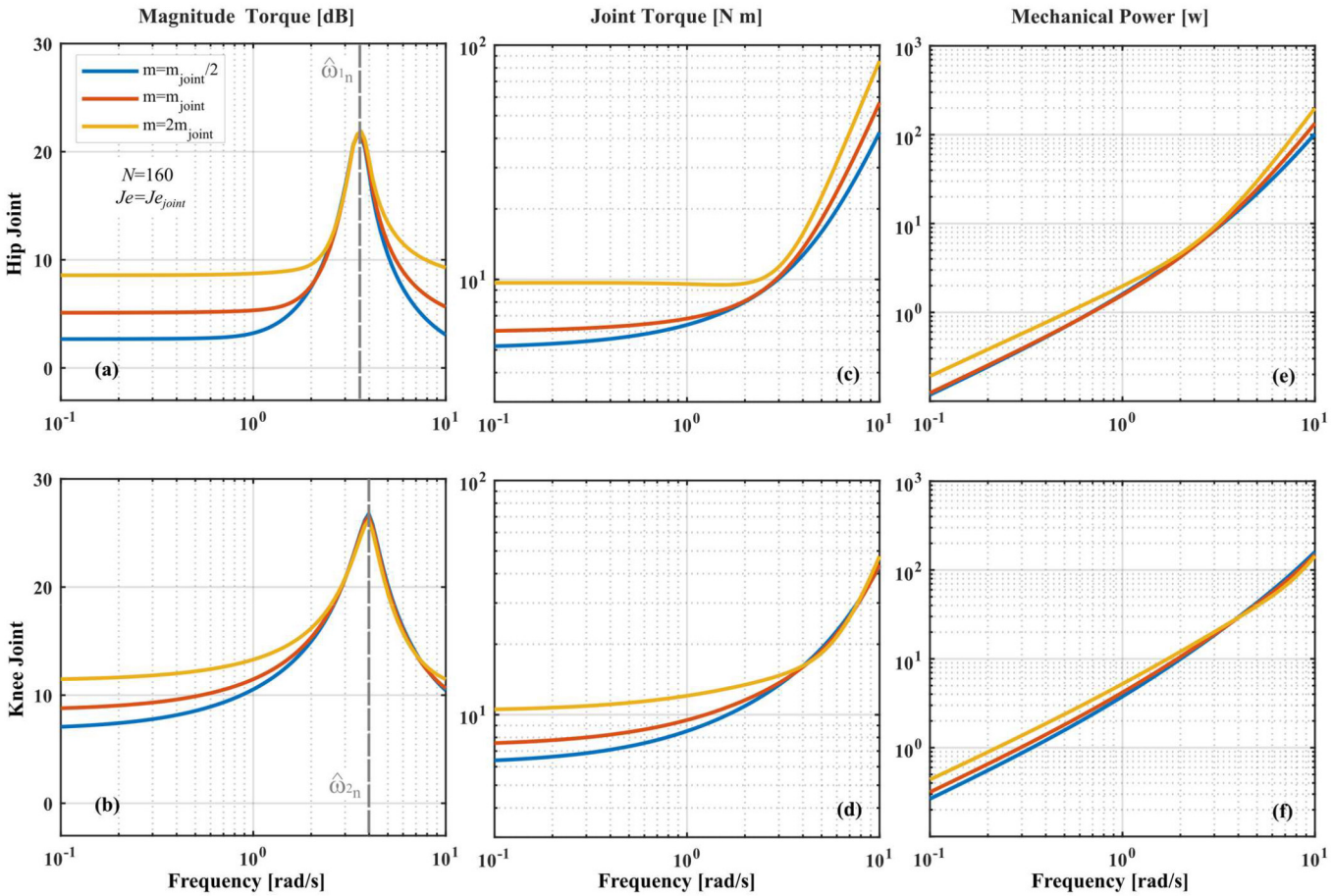

Fig. 8. The effect of the actuator's mass on the driving torques and mechanical power. While the mass changes, motor-reducer transmission ratio (N) and actuator's apparent inertia (Je) are kept as $N = 160$ and $Je = Je_{joint}$. (a) and (b) are the magnitude torques on the hip and knee joints, respectively, and $\hat{\omega}_{1n}$ and $\hat{\omega}_{2n}$ represent the hip and knee joint resonant frequencies of the ideal double-pendulum model. (c) and (d) are the resulting joint torques and (e) and (f) are the mechanical power of the hip and knee joints, respectively.

friction and reduces the required torque to move the joint. The same effect is observed on the joint mechanical power (Fig. 8 (e) and (f)), the mechanical power of the increased mass exoskeleton is even lower than the reduced one. It is worth noting that, depending on the stride frequency, an exoskeleton with greater mass can be more transparent to the user than a lighter one.

The effect of changing the actuator's reduction ratio (N) is presented in Fig. 9. The results were gathered considering the standard mass ($m_1 = m_{K_{nee}}$ and $m_2 = m_{Ankle}$) and links lengths ($l_1 = l_{Thigh}$ and $l_2 = l_{Shank}$), whereas N ranges from 30 to 160. It's easy to note that by increasing N, the magnitude torque, torque, and mechanical power increase accordingly. It is noticeable that changing the apparent inertia and friction of the actuator, due to the variation of N, produces an U-shaped torque and mechanical power curves for $N = 30, 50$ and 80. The resonant frequencies of the joints of the exoskeleton's model are lower than the ones of the ideal double-pendulum ($\hat{\omega}_{1n}$) due to the increased actuator's apparent inertia. However, the frequency of the torque valley on the knee joint is greater than $\hat{\omega}_{2n}$, so that the friction here plays a more important role than inertia in changing the minimum torque to drive the shank. As previously discussed in Fig. 4, for high frequencies ($\omega > 6$ rad/s), inertial and Coriolis effects produced by the thigh movement on the shank increase, and friction plays a role to minimize the joint torque. For greater N, the friction effect is higher, and the U-shape is not noticeable. The energetic cost to move the joints are very sensitive to the system dynamics and stride frequency, similar minimum force cost is reported by [28].

Finally, to compare the driving forces of exoskeletons with different sizes of actuators, Fig. 10 displays three combinations of mass, apparent inertia, and friction: blue line represents an exoskeleton with small and lightweight actuators ($m_1 = m_{K_{nee}}/2$ and $m_2 = m_{Ankle}/2, Je_1 = Je_{Hip}/2$ and $Je_2 = Je_{Knee}/2$), but high reduction ratio ($N = 200$). Red line is for the standard mass and apparent inertia of the ExoRoboWalker and reduction ratio $N = 100$. Yellow line represents the actuator with increased mass ($m_1 = 2m_{K_{nee}}$ and $m_2 = 2m_{Ankle}$) and apparent inertia ($Je_1 = 2Je_{Hip}$ and $Je_2 = 2Je_{Knee}$) and reduced reduction ratio $N = 50$ to simulate an exoskeleton with a bigger actuator. Remarkably, for a wide range of frequency the mechanical power (Fig. 10 (e) and (f)) to move the joints is lower for an exoskeleton with bigger actuators and low reduction ratio than for one with lightweight actuators and higher reduction ratio (0.7 to 6 rad/s

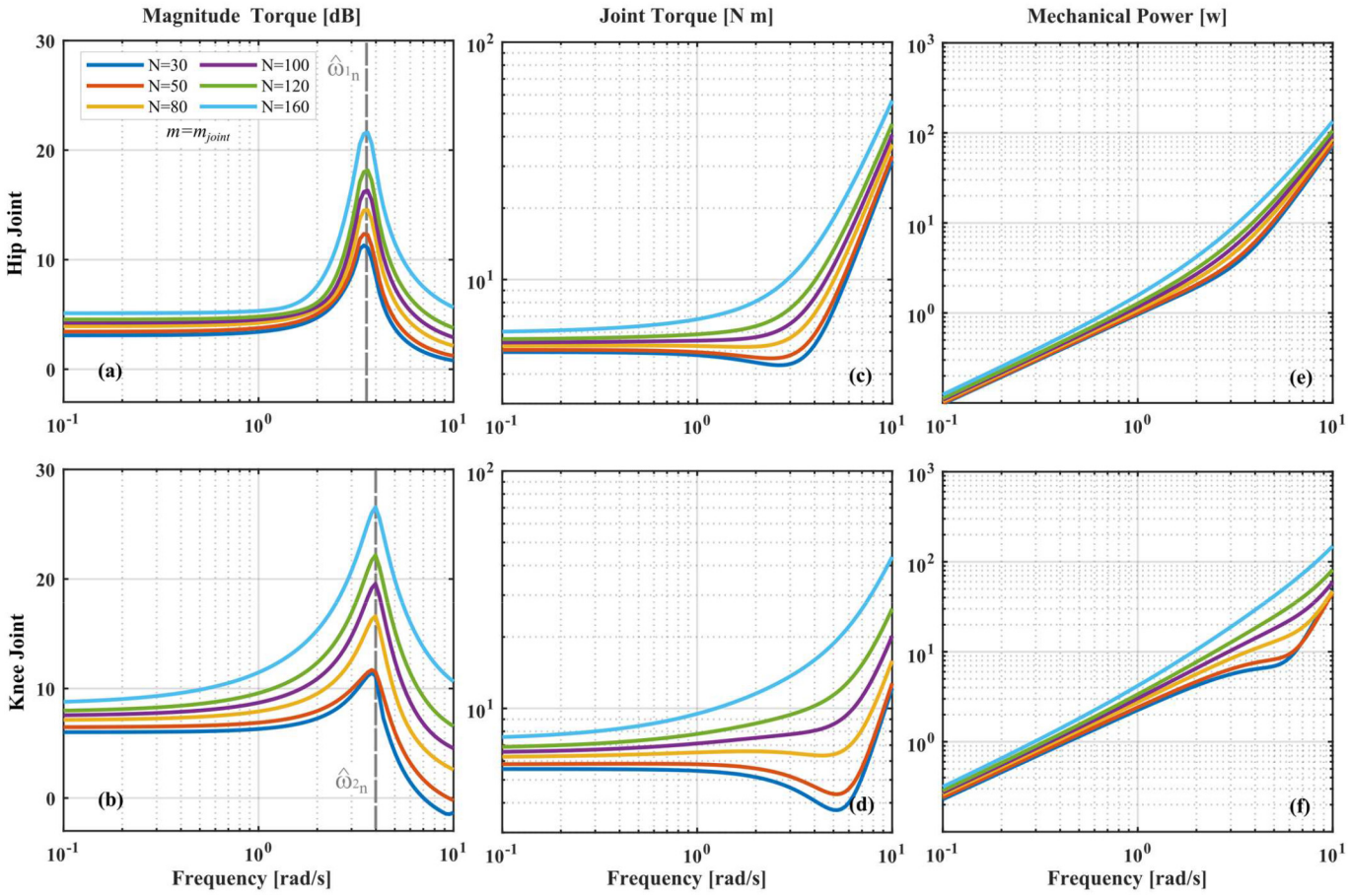

Fig. 9. Combined effect of friction and apparent inertia due to the moto-reducer transmission ratio variation on the magnitude torque of hip (a) and knee (b) joints. Joint torque of hip (c) and knee (d) joints and mechanical power (e) (hip) and (f) (knee). The actuator's mass is kept constant as m_1=$m_{K_{nee}}$ and m_2=m_{Ankle} and $\hat{\omega}_{1n}$ represents the hip joint resonant frequency of the ideal double-pendulum model and $\hat{\omega}_{2n}$ for the knee joint.

for the hip joint and 0.5 to 9 rad/s for the knee joint). The difference in mechanical power can reach 9.5 W for the hip joint and 41.6 W for the knee joint. The shape of the required joint torque graph is also strongly dependent on the actuator's mass, apparent inertia and friction. The increased mass actuator presents a valley of minimum torque near the resonant frequency (Fig. 10 (c) and (d)) and it can be lower than the reduced mass actuator by 6.9 N m (hip) and 11.6 N m (knee).

IV. Discussion

The primary interest of this investigation was to explore the effects of the actuator's mass, apparent inertia, and friction on the driving torques and mechanical power of gait training exoskeletons. Following the assistance as needed concept [9], here we argue that such exoskeletons should be designed to be transparent to the user and introduce torques only when voluntarily generated motor outputs deviate from the healthy movement [13]. However, the transparent operation of wearable robots is still an open problem with several issues to be overcome [11]–[13]. The best way to have a transparent system is designing it to minimally interfere with the user's natural gait when it is unpowered [35], then a transparent operation method can be more easily implemented.

The effect of adding mass on the leg [15], [16], [43] or on the wearable robot [17], [35] has been used as the most important criterion to investigate gait variation to design wearable systems. However, the resonant frequency of the double-pendulum, used to model the exoskeleton dynamics, play a crucial role in determining the natural stride frequency of the user wearing the robot. Previous studies [28], [44], [45] indicate the self-selected walking speed results in a minimal metabolic cost of walking and it is associated to the resonant frequency of the leg as a simple-pendulum with same mass and equivalent length of its CoM [28]. Mass, inertia, and friction integrated to the leg by wearable devices change the natural oscillation frequency of the system as well as the kinematics, dynamics and metabolic cost of walking [16], [26]. The user wearing the system will naturally try to find a new stride frequency corresponding to a minimal metabolic cost [28]. For that reason, designing a transparent system by just minimizing the user-robot interaction forces [12], [33], [34] it is not enough to avoid interfering with the user's gait.

To clarify the understanding of the actuator's mass, apparent inertia and friction effects on the driving torques and mechanical power of lower-limb exoskeletons, we introduce a simple-pendulum model plus inertia and viscous friction, presented in Fig. 11. By applying the Newton's second law for

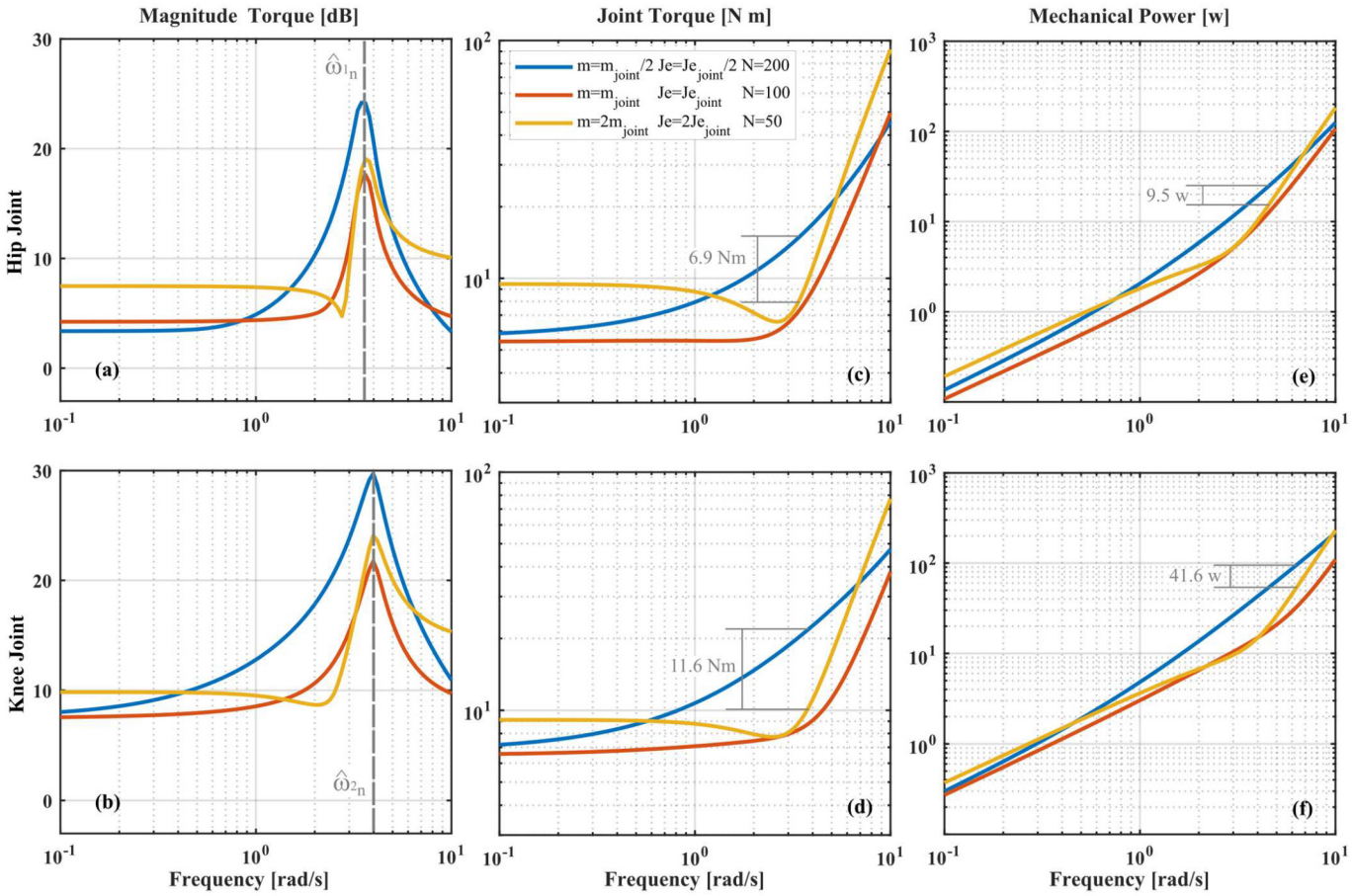

Fig. 10. Combined effect of mass, apparent inertia and friction variation on the driving forces and mechanical power as a function of the joint angular velocity. (a) and (b) are the hip and knee magnitude torque, (c) and (d) are the joint torque, and (e) and (f) the mechanical power. Blue line represents the effect of half mass and apparent inertia and transmission ratio N=200, whereas red line is the effect of standard mass and apparent inertia and N=100 and yellow line is the effect of double mass and apparent inertia and N=50.

rotational systems, the equation of motion for the pendulum is:

$$\tau = \left(ml^2 + J\right)\ddot{\theta} + b\theta + \dot{mglsin}(\theta) \tag{21}$$

where τ is the driving torque of the joint, m, l and θ are the pendulum mass, length and angle, respectively, b is the viscous friction coefficient, and J is the inertia added to the pendulum joint. Considering the free oscillating movement (τ = 0) and small angular amplitude displacement, Eq. (21) can be rewritten as:

$$\begin{cases} \ddot{\theta} + \zeta\,\dot{\theta} + {\omega_n}^2\theta = 0 \\ \zeta = \frac{b}{ml^2+J} \\ \omega_n = \sqrt{\frac{mgl}{ml^2+J}} \end{cases} \tag{22}$$

The solution for (22) is a common damped harmonic oscillator with ζ as damping coefficient and ω_n as resonant frequency. For the cases where b = 0 and J = 0, Eq. (22) can be reduced to the idealized simple-pendulum case as:

$$\ddot{\theta} + \frac{g}{l}\theta = 0 \tag{23}$$

where $\sqrt{g/l}$ is the resonant frequency of the system.

The results of the isolated effects help us to understand how the actuator's apparent inertia and friction and link length interfere with the driving torques of a gait training exoskeleton. Whereas the potential and kinetic energy of the actuator's mass and apparent inertia are conservative and can be interchanged, the damping energy due to the friction it is not. Consequently, unlike the effects of inertia, friction does not change the frequency of minimum energy cost, instead it increases the walking cost regardless the speed [31], as presented in Fig. 4. It can be reasonably well described by the simple-pendulum plus inertia and friction in Fig. 11 and Eq. (22). In this case, the resonant frequency is mainly changed by l and J, whereas friction just interferes with the pendulum damping. Moreover, as the friction is proportional to the joint velocity, it is expected that the user reduces the walking speed to minimize the walking cost, like walking in water [32]. However, it worth noting that for high frequencies, $\omega > 10$ rad/s, as presented in Fig. 7(b), $\tau<\hat{\tau}$, i.e., the joint friction minimizes the out-of-phase inertial and Coriolis effects from the thigh movement on the shank, resulting in a negative magnitude torque.

The isolated effect of the actuator's mass variation does not change the resonant frequency of the system. It can be interpreted based on the simple-pendulum model (23), since the natural oscillation frequency is regardless the system's mass. Although adding mass on the user leg increases the energy cost of walking, as discussed in [26], if weights are added on the

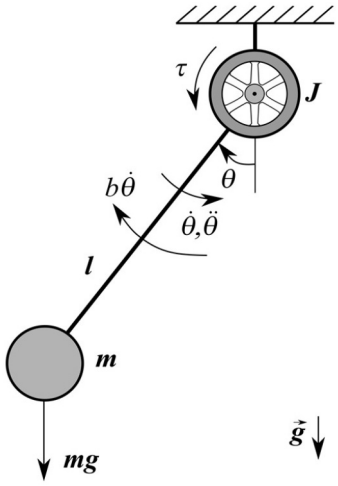

Fig. 11. Oscillating simple-pendulum model (length = l and mass = m) integrated with inertia (J) and viscous friction ($b\dot{\theta}$).

equivalent center of mass of the leg, it will not play a crucial role on the user's kinematics and natural stride frequency. This is in agreement with the experiments carried out by [15]–[17], [26]. However, the effect of adding inertia to the joint, but not changing its mass, is quite district. Increasing the actuator's apparent inertia reduces the resonant frequency of the system, as shown in Fig. 5. This effect can also be well explained by the simple-pendulum model with friction and inertia, Eq. (22), where the resonant frequency of the system is inversely proportional to the joint inertia. It means that, increasing the apparent inertia of the user's joint will reduce their economical stride frequency. The same effect was observed by [28] by adding weights on the subject's leg far from the joint center of rotation. From a transparent exoskeleton point of view, it means that the inertia of the robot plays a more important role on the gait kinematics of the user than mass. However, from a metabolic cost point of view, increased mass or inertia can have the same effect depending on the stride frequency [26], [42].

The isolated effect of the exoskeleton's link length variation, shown in Fig. 6, can be interpreted as the actuator's CoM location in a gait trainer exoskeleton. Increased length of the links reduces the minimum torque frequency and increases the inertial, Coriolis, and gravitational forces of the joint. The effect of changing the length of thigh (red and blue lines) and shank (purple and yellow lines) is similar on the magnitude torque of the hip joint, but the associated effect of changing l_{Thigh} and l_{Shank} (light blue and green line) are more important. However, the knee joint is more sensitive to the shank length variation. The simple-pendulum model can be used to better understand these behaviors. Increased l reduces the natural frequency of the pendulum, which is in accordance with [28], [42], [46], and increases the required torque to move it (21). Moreover, it is known that bringing the added weights close to the hip reduces the metabolic cost of walking and the torques on the joints [16], [47].

It can be easily seen in Fig. 7 that the frequency of the minimum torque on the hip joint varies more with the associated variation of l_{Thigh} and l_{Shank} (green squares) than with changes of l_{Shank} (black stars), l_{Thigh} (magenta x-marks) or actuator's inertia (blue circles). On the other hand, the effects of minimum torque frequency on the knee joint for links length variation look similar. In a first glance, it seems to be in disagreement with the study developed by [15], where they investigated the effect of adding mass on children's leg on the kinematics and spatiotemporal parameters of walking. No significant variation was observed on the stride frequency of self-selected speed. However, a detailed look at their experimental protocol revels that the position of the added mass was exactly at the equivalent CoM of the leg, right below the knee. It means that no variation of the pendulum length was caused by the added mass and so no variation on the resonant frequency. The kinematics variation observed was associated to the orthosis constraints imposed to the children's leg and not by the added mass, as argued by the authors. Remarkably, the effect of increasing the actuator's friction on the knee joint torque, denoted by $N = 100R$ (red $+-$marks) is inverted compared to the others, i.e., increased friction increases the minimum torque frequency. It could be wrongly interpreted as increasing the actuator friction would increase the resonant frequency of the system and so the natural stride frequency of the user. However, this minimum torque is just observed in the knee joint for high frequencies, due to the out-of-phase Coriolis and inertial torques from the hip joint that is minimized by the friction, as previously explained.

The combined effects of mass, inertia and friction are quite interesting. It is natural to think that the mass of the exoskeleton is the most important criterion for transparent operation and over the years it has been used to reduce the impact on the user's kinematics [15]–[17], [43]. However, our data have shown that the effects of the apparent inertia and friction, created by the high reduction ratio, typically used in exoskeletons [11], [13], [19], [20], also plays an essential role on the user's gait. In Fig. 8 (c) and (d) it is possible to check the absolute torques on the joints and, depending on the oscillation frequency of the system, the actuator's mass has little importance, mainly for the knee joint. The results of mass variation are even more interesting when we observe the joint mechanical power. It is worth noting that the joint mechanical power has been associated with the metabolic cost of walking [26] and energy consumption of the system [49]. Remarkably, a greater actuator's mass can require less mechanical power on the knee joint. It is not possible to be noticed when the effects of inertia and friction are neglected. Clearly, in a general analysis, greater mass requires greater torque and mechanical power of the joint. However, for a system where the friction is not neglected, great mass and inertia create greater conservative forces mainly in high frequencies, so the effect of dissipative forces becomes less important. Such argument can also be explained by the simple pendulum model with friction and inertia. The damping coefficient ζ (22) is inversely proportional to the mass. It means that the effect of friction on the driving toques becomes more important for lightweight exoskeletons.

This arguing agrees with the results shown in Fig. 9, where the effects of increased reduction ratio ranging from 30 to 160 were evaluated for the same actuator's mass ($m_1 = m_{Knee}$

and $m_2 = m_{Ankle}$). High reduction ratio produces high friction and apparent inertia in the actuator and requires high torque and mechanical power to move the joints. Interestingly, an U-shaped curve of minimum joint torque is observed for low reduction ratio ($N = 30$, 50 and 80). However, it is not apparent in high friction actuators. The behavior is supported by previous studies [28], [46], where the authors argued that the effect of the stride frequency becomes crucial to find a minimal walking cost for low non-conservative forces and greater mass. It means that low reduction ratio actuators can be used to adjust the stride frequency of the user for a low metabolic cost. High reduction ratio actuators, on the other hand, produce results like those where people walk in water [30]–[32]. The drag forces of the water and apparent body-weight reduction reduce the conservative forces and improve the damping ones, so that the effect is a lower stride frequency and walking velocity, but not lower joint range of motion [32].

Finally, the results shown in Fig. 10 are remarkable. For a wide range of operation frequencies, the high mass and low friction actuators (yellow line) presented considerably lower joint torque and mechanical power than the low mass and high reduction ratio actuators (blue line). In general, better results are observed for the standard actuator's mass and apparent inertia and considering the friction form a $N = 100$ harmonic-drive. The increased mass and low friction improved the U-shaped curve for torque (Fig. 10(c) and (d)) and mechanical power (Fig. 10(e) and (f)) in both joints. It means that it is easier to adjust the stride frequency of the system to find a low metabolic cost of walking when the conservative forces are greater and the dissipative ones are lower [28], [46].

These findings have several implications for lower-limb gait training exoskeletons: First of all, the actuator's mass and center of mass position does play an important role on the driving torques and mechanical power, however to understand the real behavior of the analyzed system, friction and apparent inertia should be suitably integrated to it. Secondly, to design a transparent lower-limb wearable robotic system, the stride frequency should be taken into account to adjust the system's parameters to a minimum metabolic cost of walking. In this way, it will be easier to make the system transparent to the user. Lastly, since friction damps the lower-limb movements and joint apparent inertia reduces the stride frequency of walking, the actuator's reduction ratio should be as low as possible to reduce its associated friction and apparent inertia. Direct-drive [50] or quasi-direct-drive actuators [22] located near the hip [16], [47], even with high mass, seem to be the best option to minimally interfere with the user's gait.

V. Conclusion

This article presented an analysis of the required driving torques and mechanical power for lower-limb gait training exoskeletons under a wide range variation of the actuator's mass, apparent inertia, friction, and thigh/shank length. To make this analysis possible, we built a model of the ExoRoboWalker, a lightweight six-degree-of-freedom lower-limb exoskeleton for overground training, using the double-pendulum approach integrated to the actuator's impedance. Joint apparent inertia was considered decoupled from the actuator's mass and friction was introduced by the Rayleigh's dissipation function on the robot's Lagrangian. The results were displayed in two main categories: isolated effect and combined effect of actuator's mass, apparent inertia, friction, and thigh/shank length. The isolated analysis was focused to investigate how such variables interfere with the joint frequency of minimum torque. It was important to help understand in what manner the exoskeleton can interfere with the user's natural stride frequency. The combined effect, on the other hand, remarkably revealed that a heavier exoskeleton with low transmission ratio, can require lower joint torques and mechanical power than a lighter one with high transmission ratio, depending on the stride frequency. It means that, depending on the exoskeleton's actuator design, a heavier system can be more transparent to the user than a lighter one. These findings are essential to help improve designs of lower-limb wearable robots for gait training, and motivate us to explore new analysis and experiments in future works to improve the transparency of such systems.

References

[1] D. Shi, W. Zhang, W. Zhang, and X. Ding, "A review on lower limb rehabilitation exoskeleton robots," *Chin. J. Mech. Eng.*, vol. 32, no. 1, p. 74, Aug. 2019.

[2] I. Díaz, J. J. Gil, and E. Sanchez, "Lower-limb robotic rehabilitation: Literature review and challenges," *J. Robot.*, vol. 2011, 2011, Art. no. 759764. [Online]. Available: https://doi.org/10.1155/2011/759764

[3] I. Borggraefe *et al.*, "Robotic-assisted treadmill therapy improves walking and standing performance in children and adolescents with cerebral palsy," *Eur. J. Paediatr. Neurol.*, vol. 14, no. 6, pp. 496–502, 2010.

[4] C. Hartigan *et al.*, "Mobility outcomes following five training sessions with a powered exoskeleton," *Top Spinal Cord Injury Rehabil.*, vol. 21, no. 2, pp. 93–99, 2015.

[5] A. Tsukahara *et al.*, "Sit-to-stand and stand-to-sit transfer support for complete paraplegic patients with robot suit HAL," *Adv. Robot.*, vol. 24, no. 11, pp. 1615–1638, Apr. 2012.

[6] K. A. Strausser and H. Kazerooni, "The development and testing of a human machine interface for a mobile medical exoskeleton," in *Proc. IEEE/RSJ Int. Conf. Intell. Robots Syst.*, 2011, pp. 4911–4916.

[7] T. Yan, M. Cempini, C. M. Oddo, and N. Vitiello, "Review of assistive strategies in powered lower-limb orthoses and exoskeletons," *Robot. Auton. Syst.*, vol. 64, pp. 120–136, Feb. 2015.

[8] A. Mutlu, K. Krosschell, and D. G. Spira, "Treadmill training with partial body-weight support in children with cerebral palsy: A systematic review," *Dev. Med. Child Neurol.*, vol. 51, no. 4, pp. 268–275, Apr. 2009.

[9] E. T. Wolbrecht, V. Chan, D. J. Reinkensmeyer, and J. E. Bobrow, "Optimizing compliant, model-based robotic assistance to promote neurorehabilitation," *IEEE Trans. Neural Syst. Rehabil. Eng.*, vol. 16, no. 3, pp. 286–297, Jun. 2008.

[10] M. J. Claros, R. Soto, J. L. Gordillo, J. L. Pons, and J. L. Contreras-Vidal, "Robotic assistance of human motion using active-backdrivability on a geared electromagnetic motor," *Int. J. Adv. Robot. Syst.*, vol. 13, no. 2, p. 40, Mar. 2016.

[11] R. Mendoza-Crespo, R. Soto, and J. L. Pons, "Transparent mode for lower limb exoskeleton," in *Wearable Robotics: Challenges and Trends* (Biosystems and Biorobotics), J. González-Vargas, J. Ibâñez, J. Contreras-Vidal, H. van der Kooij, and J. Pons, Eds., vol. 16. Cham, Switzerland: Springer, 2017. [Online]. Available: https://doi.org/10.1007/978-3-319-46532-6_69

[12] D. Zanotto, T. Lenzi, P. Stegall, and S. K. Agrawal, "Improving transparency of powered exoskeletons using force/torque sensors on the supporting cuffs," in *Proc. IEEE 13th Int. Conf. Rehabil. Robot. (ICORR)*, 2013, pp. 1–6.

[13] R. M. Andrade, S. Sapienza, and P. Bonato, "Development of a 'transparent operation mode' for a lower-limb exoskeleton designed for children with cerebral palsy," in *Proc. IEEE 16th Int. Conf. Rehabil. Robot. (ICORR)*, 2019, pp. 512–517, doi: 10.1109/ICORR.2019.8779432.

[14] B. Na, J. Bae, and K. Kong, "Back-drivability recovery of a full lower extremity assistive robot," in *Proc. 12th Int. Conf. Control Autom. Syst.*, 2012, pp. 1030–1034.
[15] S. Rossi, A. Colazza, M. Petrarca, E. Castelli, P. Cappa, and H. I. Krebs, "Feasibility study of a wearable exoskeleton for children: Is the gait altered by adding masses on lower limbs?" *PLOS ONE*, vol. 8, no. 9, Apr. 2013, Art. no. e73139.
[16] R. C. Browning, J. R. Modica, R. Kram, and A. Goswami, "The effects of adding mass to the legs on the energetics and biomechanics of walking," *Med. Sci. Sports Exerc.*, vol. 39, no. 3, pp. 515–525, Mar. 2007.
[17] X. Jin, Y. Cai, A. Prado, and S. K. Agrawal, "Effects of exoskeleton weight and inertia on human walking," in *Proc. IEEE Int. Conf. Robot. Autom. (ICRA)*, May 2017, pp. 1772–1777.
[18] S. L. Barnett, A. M. Bagley, and H. B. Skinner, "Ankle weight effect on gait: Orthotic implications," *Orthopedics*, vol. 16, no. 10, pp. 1127–1131, Oct. 1993.
[19] M. Bortole *et al.*, "The H2 robotic exoskeleton for gait rehabilitation after stroke: Early findings from a clinical study," *J. NeuroEng. Rehabil.*, vol. 12, no. 1, p. 54, Jun. 2015.
[20] E. Garcia, J. Sancho, D. Sanz-Merodio, and M. Prieto, "ATLAS 2020: The pediatric gait exoskeleton project," in *Human-Centric Robotics*. Singapore: World Sci., 2017, pp. 29–38.
[21] S. V. Sarkisian, M. K. Ishmael, G. R. Hunt, and T. Lenzi, "Design, development, and validation of a self-aligning mechanism for high-torque powered knee exoskeletons," *IEEE Trans. Med. Robot. Bionics*, vol. 2, no. 2, pp. 248–259, May 2020
[22] G. Lv, H. Zhu, and R. D. Gregg, "On the design and control of highly backdrivable lower-limb exoskeletons: A discussion of past and ongoing work," *IEEE Control Syst. Mag.*, vol. 38, no. 6, pp. 88–113, Dec. 2018.
[23] R. M. Andrade, A. B. Filho, C. B. S. Vimieiro, and M. Pinotti, "Optimal design and torque control of an active magnetorheological prosthetic knee," *Smart Mater. Struct.*, vol. 27, no. 10, Sep. 2018, Art. no. 105031, doi: 10.1088/1361-665X/aadd5c.
[24] H. Zhu, J. Doan, C. Stence, G. Lv, T. Elery, and R. Gregg, "Design and validation of a torque dense, highly backdrivable powered knee-ankle orthosis," in *Proc. IEEE Int. Conf. Robot. Autom.*, May 2017, pp. 504–510.
[25] S. Seok *et al.*, "Design principles for energy-efficient legged locomotion and implementation on the MIT Cheetah robot," *IEEE/ASME Trans. Mechatrons*, vol. 20, no. 3, pp. 1117–1129, Jun. 2015.
[26] T. D. Royer and P. E. Martin, "Manipulations of leg mass and moment of inertia: Effects on energy cost of walking," *Med. Sci. Sports Exerc.*, vol. 37, no. 4, pp. 649–656, Apr. 2005.
[27] J. M. Finley, A. J. Bastian, and J. S. Gottschall, "Learning to be economical: The energy cost of walking tracks motor adaptation," *J. Physiol.*, vol. 591, no. 4, pp. 1081–1095, Feb. 2013.
[28] K. G. Holt, J. Hamill, and R. O. Andres, "The force-driven harmonic oscillator as a model for human locomotion," *Human Movement Sci.*, vol. 9, no. 1, pp. 55–68, Feb. 1990.
[29] A. D. Kuo, "A simple model of bipedal walking predicts the preferred speed-step length relationship," *J. Biomech. Eng.*, vol. 123, no. 3, pp. 264–269, Jun. 2001, doi: 10.1115/1.1372322.
[30] K. Masumoto, T. Shono, S.-I. Takasugi, N. Hotta, K. Fujishima, and Y. Iwamoto, "Age-related differences in muscle activity, stride frequency and heart rate response during walking in water," *J. Electromyogr. Kinesiol.*, vol. 17, no. 5, pp. 596–604, Oct. 2007.
[31] K. Masumoto, T. Shono, N. Hotta, and K. Fujishima, "Muscle activation, cardiorespiratory response, and rating of perceived exertion in older subjects while walking in water and on dry land," *J. Electromyogr. Kinesiol.*, vol. 18, no. 4, pp. 581–590, Aug. 2008.
[32] A. M. F. Barela, S. F. Stolf, and M. Duarte, "Biomechanical characteristics of adults walking in shallow water and on land," *J. Electromyogr. Kinesiol.*, vol. 16, no. 3, pp. 250–256, Jun. 2006.
[33] F. Just *et al.*, "Exoskeleton transparency: Feed-forward compensation vs. Disturbance observer," *Automatisierungstechnik*, vol. 66, no. 12, pp. 1014–1026, Dec. 2018.
[34] E. H. F. van Asseldonk, J. F. Veneman, R. Ekkelenkamp, J. H. Buurke, F. C. T. van der Helm, and H. van der Kooij, "The effects on kinematics and muscle activity of walking in a robotic gait trainer during zero-force control," *IEEE Trans. Neural Syst. Rehabil. Eng.*, vol. 16, no. 4, pp. 360–370, Aug. 2008.
[35] V. Bartenbach, D. Wyss, D. Seuret, and R. Riener, "A lower limb exoskeleton research platform to investigate human-robot interaction," in *Proc. IEEE Int. Conf. Rehabil. Robot. (ICORR)*, Singapore, 2015, pp. 600–605.
[36] I. Cajigas, A. Koenig, G. Severini, M. Smith, and P. Bonato, "Robot-induced perturbations of human walking reveal a selective generation of motor adaptation," *Sci. Robot.*, vol. 2, no. 6, May 2017, Art. no. eaam7749.
[37] C. M. Mitschka, M. H. Terra, and A. A. G. Siqueira, "Derivation of a Markovian Controller for an exoskeleton by overcome the benchmarks of a single and double inverted pendulum," in *Proc. 54th IEEE Conf. Decis. Control (CDC)*, 2015, pp. 5061–5066.
[38] B. Hwang and D. Jeon, "A method to accurately estimate the muscular torques of human wearing exoskeletons by torque sensors," *Sensors*, vol. 15, no. 4, pp. 8337–8357, Apr. 2015.
[39] U. Yerlikaya and T. Balkan, "Identification of viscous and coulomb friction in motion constrained systems," in *Proc. IEEE/ASME Int. Conf. Adv. Intell. Mechatronics (AIM)*, 2018, pp. 91–96.
[40] J. L. Pons, *Wearable Robots: Biomechatronic Exoskeletons*. Chichester, U.K.: Wiley, Mar. 2008.
[41] E. Minguzzi, "Rayleigh's dissipation function at work," *Eur. J. Phys.*, vol. 36, no. 3, Mar. 2015, Art. no. 035014.
[42] J. Doke, J. M. Donelan, and A. D. Kuo, "Mechanics and energetics of swinging the human leg," *J. Exp. Biol.*, vol. 208, no. 3, pp. 439–445, Feb. 2005.
[43] J. H. Meuleman, E. H. van Asseldonk, and H. van der Kooij, "The effect of directional inertias added to pelvis and ankle on gait," *J. NeuroEng. Rehabil.*, vol. 10, no. 1, p. 40, Apr. 2013, doi: 10.1186/1743-0003-10-40.
[44] P. N. Kugler and M. T. Turvey, *Information, Natural Law, and the Self-Assembly of Rhythmic Movement; Theoretical and Experimental Investigations*. Hillsdale, NJ, USA: Erlbaum, 1987.
[45] J. M. Workman and B. W. Armstrong, "Metabolic cost of walking: Equation and model," *J. Appl. Physiol.*, vol. 61, no. 4, pp. 1369–1374, Oct. 1986.
[46] P. N. Kugler, J. A. S. Kelso, and M. T. Turvey, "1 On the concept of coordinative structures as dissipative structures: I. Theoretical Lines of convergence," in *Advances in Psychology*, G. E. Stelmach and J. Requin, Eds., vol. 1. North Holland, The Netherlands: Elsevier, 1980, pp. 3–47.
[47] J. Kim *et al.*, "Reducing the metabolic rate of walking and running with a versatile, portable exosuit," *Science*, vol. 365, no. 6454, pp. 668–672, Aug. 2019, doi: 10.1126/science.aav7536.
[48] R. M. Andrade, A. B. Filho, C. B. S. Vimieiro, and M. Pinotti, "Evaluating energy consumption of an active magnetorheological knee prosthesis," in *Proc. 19th Int. Conf. Adv. Robot. (ICAR)*, Dec. 2019, pp. 75–80, doi: 10.1109/ICAR46387.2019.8981642.
[49] R. M. Andrade, J. S. R. Martins, M. Pinotti, A. B. Filho, and C. B. S. Vimieiro, "Novel active magnetorheological knee prosthesis presents low energy consumption during ground walking," *J. Intell. Mater. Syst. Struct.*, to be published, doi: 10.1177/1045389X20983923.
[50] G. Kenneally, A. De, and D. E. Koditschek, "Design principles for a family of direct-drive legged robots," *IEEE Robot. Autom. Lett.*, vol. 1, no. 2, pp. 900–907, Jul. 2016.

Rafhael M. Andrade (Member, IEEE) received the B.S. and M.S. degrees in mechanical engineering from the Federal University of Espírito Santo (UFES), Vitória, Brazil, in 2009 and 2013, respectively, and the Ph.D. degree in mechanical engineering from the Federal University of Minas Gerais, Belo Horizonte, Brazil, in 2018.

He has been a Professor with the Department of Mechanical Engineering, UFES since 2013, and a Research Collaborator with the Department of Physical Medicine and Rehabilitation, Harvard Medical School, Spaulding Rehabilitation Hospital. He is a Coordinator of the UFES Robotics and Biomechanics Laboratory and works as a Collaborating Researcher with LabBio, Bioengineering Laboratory, Federal University of Minas Gerais. His research interests include the design and control of prosthesis and exoskeleton, biomechanics, biomechatronics, and smart materials.

Paolo Bonato (Senior Member, IEEE) received the M.S. degree in electrical engineering from the Politecnico di Torino, Turin, Italy, in 1989, and the Ph.D. degree in biomedical engineering from the Universita di Roma "La Sapienza," Rome, Italy, in 1995.

He serves as a Director of the Motion Analysis Laboratory, Spaulding Rehabilitation Hospital, Boston, MA, USA, and he is an Associate Professor with the Department of Physical Medicine and Rehabilitation, Harvard Medical School, Boston. His research interest is focused on rehabilitation technology with a special emphasis on mobile health technology and rehabilitation robotics.